

Radome Design and Experimental Characterization of Scattering and Propagation Properties for Atmospheric Radar Applications

José D. Díaz^{1,2,3}, Jorge L. Salazar^{2,3}, Alessio Mancini⁴, Jose G. Colom¹

¹University of Puerto Rico at Mayagüez (UPRM) ²National Center for Atmospheric Research (NCAR)

³Advanced Radar Research Center (ARRC), University of Oklahoma (OU)

⁴Colorado State University (CSU)

Abstract – In this paper an experimental approach to accurately characterize the performance of a wet radome is discussed. The design, fabrication, and characterization of the propagation and scatter properties of seven-layer radome is presented. The circuitual equivalent transmission line method was used to obtain the theoretical performance. Simulation performed in HFSS and measured results obtained in a customized RF chamber were used to validate the method proposed. The radome skin surface was implemented with non-hydrophobic, hydrophobic, and super-hydrophobic materials. Characterization of wet radome was evaluated as function of the radome geometry, position, and material. Good agreement were found between the theoretical, simulated, and measured results.

Index Terms – Radome, dual-pol, transmission line model, wet radome.

I. INTRODUCTION

For operational radar systems, the radome is an essential component that protects the radar against the rain, pollution, dust, temperature, etc. Radome helps to reduce the operational cost since it minimizes the wind load requirements, as a consequence, the need of heavy and expensive pedestals. Radar equipment under a radome keeps a nominal temperature that facilitates the operation and maintenance, improves the life cycle cost of the system Walton (1970). One adverse effect of the radome is the performance degradation of radio signals when they operate in the presence of water or ice. Water accumulated on the radome surface can significantly affect the radar signal. Depending on the frequency of operation, rain, wind conditions, shape, and

materials, a radome can significantly attenuate, reflect, and depolarize the radar or communication signals. For frequencies below S-band, the impact of wet radomes is relatively small and could not be considered critical for radar operation, see Table 1 in Salazar et al. (2014). However, for higher frequencies water formation on the radome surface can significantly deteriorate the transmit and receive signals (Gibble (1964), Fenn (1997), Crane (2002)). Salazar in Salazar et al. (2014) formulate an analytical method for evaluating the electrical performance of a radome for a dual-polarized phased-array antenna under rain conditions. Attenuation, reflections, and induced cross polarization are evaluated for different rainfall conditions and radome types. The authors present a model for estimating the drop size distribution on a radome surface based on skin surface material, area, inclination, and rainfall rate. Then, a multilayer radome model based on the transmission-line-equivalent circuit model is used to characterize the radome's scattering parameters. In this paper we present the characterization of the propagation and scatter properties of a seven-layer radome when the radome is dry. Characterization of the critical angle for wet-skin radome materials as function of surface and geometry of the radome is also presented.

II. MULTILAYER RADOME MODEL

A. Dry Radome

To evaluate the performance of a multilayer radome structure in dry conditions, a well-known mathematical model based on the equivalent transmission line method is used (Hirsch and Grove (1988)). This basic model was expanded for a multilayer medium with seven-dielectric layers and performance of the reflection and transmission coefficient as function of the incident angle and frequency has been considered. In Fig. 1, the representation

José D. Díaz is a former student from the UPRM who is now with ARRC as a graduate student in the ECE department at OU. This research was performed during the Summer of 2014 while the author participated in the SUPER program in NCAR Earth Observing Laboratory and finished in ARRC at OU, 3190 Monitor Ave., Norman, OK 73019. E-mail: jdiaz@ou.edu

The National Center for Atmospheric Research is sponsored by the National Science Foundation. This work was sponsored by NSF Grant M0904552.

of the seven-layer radome with a transmission line model is presented. The radome was built using the following materials: 2 layers of Teflon S240 ($\epsilon_r = 2.1$, $\tan \delta = 0.001$), 2 layers of Rohacell 31HF ($\epsilon_r = 1.04$, $\tan \delta = 0.0017$), and 3 layers of Epoxy Glue ($\epsilon_r = 5.51$, $\tan \delta = 0.008$). The thickness of the materials used to built the radome were: Teflon S240 20 mils, Epoxy glue 2 mils (6 mils in total), and Rohacell 31HF 250 and 500 mils respectively.

Assuming an incident plane wave in medium 1, the formulation for the transmission and reflection coefficients for a parallel (horizontal) and orthogonal (vertical) polarization can be represented in Eqs. (10) to (16) in Salazar et al. (2014). The transmitted signal in a multilayer radome (7-layers) can be estimated using Eq. (10). The impedance characteristic of each layer can be estimated using Eq. (11). In this expression t_n represents the thickness of each radome layer. The reflections (Γ_H and Γ_V) and transmission coefficients (T_H and T_V) for H and V polarization in each layer can be obtained by the expressions (14) and (15) in Salazar et al. (2014).

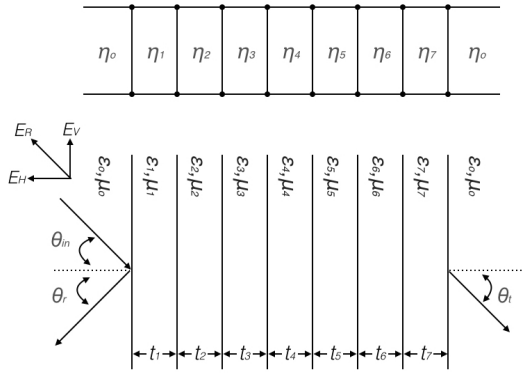


Figure 1: Representation of seven layer radome for transmission line equivalent analysis

In order to validate the theoretical results performed in MatLab, the seven-layer radome was modeled using the 3-D Finite Element Method in HFSS. Master-slave boundary condition using Floquets ports is used to model the seven-layer radome. The theoretical results compared with simulated results in HFSS of the seven-radome structures are presented in the Fig. 3. Very close agreements between both results were obtained for the transmission and reflection coefficient as function of frequency and incident angle.

B. Experimental Results

A customized RF scanner to measure the transmission and reflection coefficients for vertical and horizontal polarization as function of incident angle and frequency was implemented. The RF scanner is illustrated in Fig. 2c and d. This RF scanner consist of a rotary table that provides a high resolution for tilting the materials under test (MUT). To measure the scattering properties of the

MUT, two antennas, one for transmit and the other for receive, were used. The antennas are interconnected with a Agilent Vector Analyzer (VNA). Labview interface was designed to control both the VNA and the rotary table. It saves the S-parameters collected for each incident angle and for a range of frequency (8.7 GHz to 11.7 GHz). In order to avoid contamination from reflections in the room, microwave absorbers that suppress reflections up to 40 dB were used. The antennas used were customized antennas, especially designed to provide 13° beam-width and small far-field distance. The reason of the small beam-width, small effective aperture, and small far-field distance is to minimize the size of the scanner and the size of the sample. Fig. 2b shows a representation of the transmit antenna and MUT. At large incident angles ($> 60^\circ$) coupling between Tx and Rx antenna can affect the accuracy of the test. Fig. 2c and d shows a picture of two setups used for this experiment. Better results were obtained when the metal enclosure is used (Fig. 2d).

The Fig. 3 presents the experimental results overlapped with theoretical (in MatLab) and simulations (HFSS). Excellent agreements were found for S-parameters as function frequency. However, when the results are compared as function of incident angle, good agreements were found for incident angles $\leq 60^\circ$. The reason of this is the small sample is used. At incident angles larger than 60° , the effective aperture is smaller and coupling between the transmit and receive antenna introduce errors in the measurements.

III. WET RADOME MODEL

Most designs of antenna radomes for weather applications include a water-repellent surface (hydrophobic and superhydrophobic) to prevent water film formation or rivulets. This is an effective solution to reduce attenuation, reflections, and depolarization of the radar signals. Fig. 4 illustrates an example of water formation in a non-hydrophobic and hydrophobic surface and also the difference of a advancing contact angle of a non-hydrophobic, hydrophobic, and super-hydrophobic radome surfaces. A model that includes the drop size distribution of a radome with water-repellent surfaces was proposed by Salazar (Salazar et al. (2014)), to estimate the drop size distribution in a tilted radome surface. The method use a mathematical expression (Eq. 7 at (Salazar et al. (2014)) that estimate the critical angle. This angle represents the angle where the gravity force defeats the surface tension of the droplet on a given tilted surface. The model proposed use this mathematical expression for better estimation of the drop size distribution of the in a radome surface as function of the surface properties of the skin material and geometry of the radome. In this section experimental characterization of the critical angle of the droplets in the two most common hydrophobic and super-hydrophobic materials were performed. For the hydrophobic and for the super-hydrophobic materials, GoreTex and Hirec 100 were used respectively.

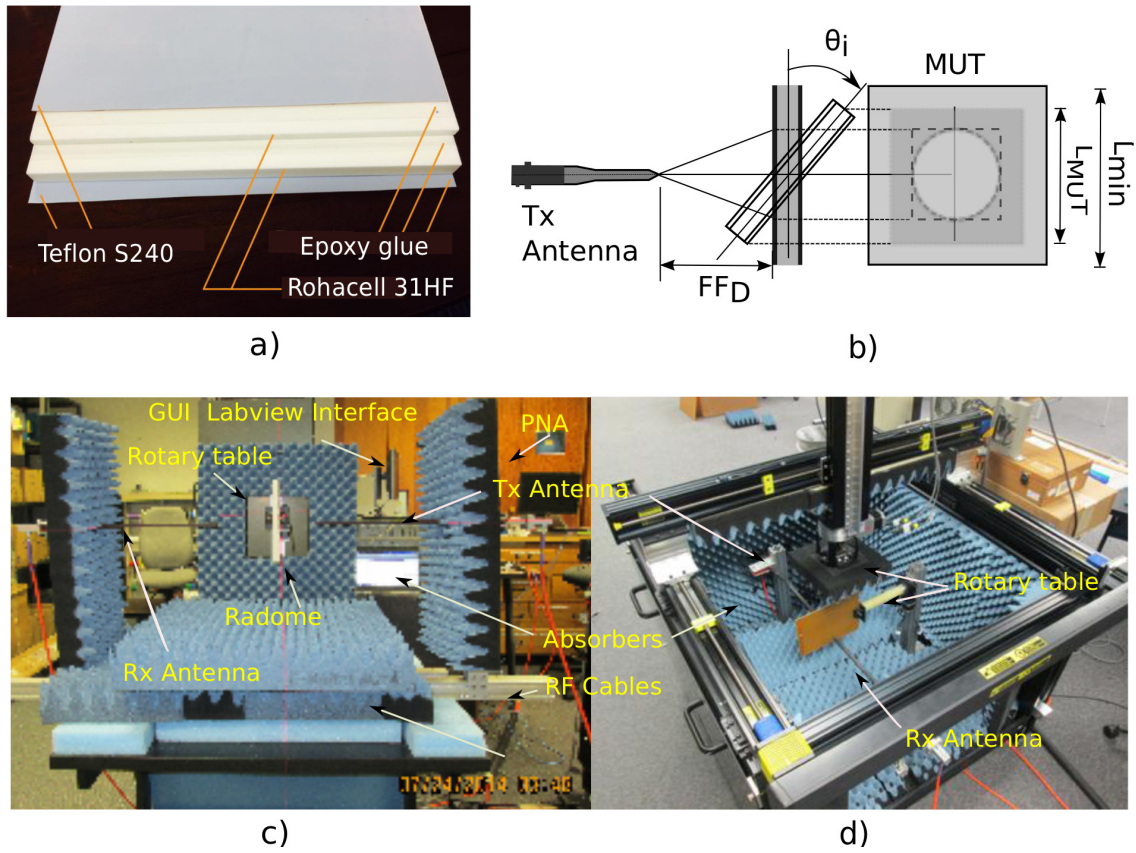


Figure 2: Radome materials under test and experimental setups.

In order to characterize the critical angle of the GoreTex and Hirec 100, samples of both materials were exposed to artificial rain. Both samples were tilted continuously from 0° to 90° using an automated rotary table and a high definition camera which took pictures every 10° as it is illustrated in Fig. 6. The figure shows the drop size distribution of Gore Tex and Hirec 100 for $0^\circ, 10^\circ, 20^\circ, 30^\circ, 40^\circ$ and 60° respectively. As it was expected, the largest droplets were removed faster in Hirec 100 than in Gore Tex. A small number of remanent droplets is observed for Gore Tex at 60° in comparison with Hirec 100. Fig. 5 presents the overlapped results of the theoretical model presented in Salazar et al. (2014) and the results obtained in this experiment. Good agreement were found for Gore Tex material however

is not the case for Hirec100 material. Based on this results shows that material is to performing as it was expected, one possible explanation is the sample was not new and It was tested several times. According to Salazar Salazar et al. (2014) and Weigand (1973), the lifetime of hydrophobic and super hydrophobic surfaces presents significant performance degradation over time. Several studies (Kurri and Huuskonen (2008) and Kurri and Huuskonen (2008)) have reported that those materials are very sensitive to pollution, dirt, sand, rain, and ice erosion. Significant degradation of the water contact angle has been observed in a short period of 4 to 6 months; after that, the radome surface requires maintenance or replacement.

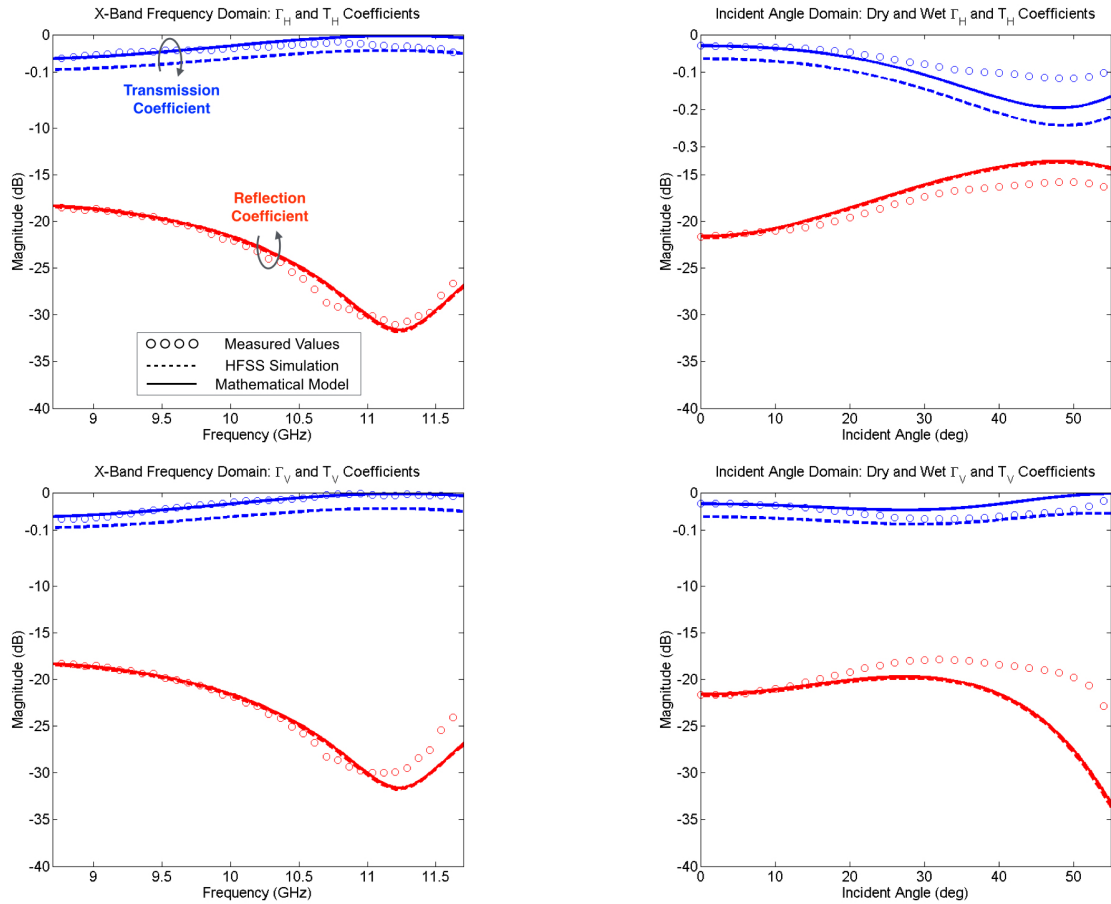


Figure 3: Reflections and Transmission coefficients for electric fields in vertical and horizontal polarizations. Red curves represent the reflection coefficients and blue curves the transmission coefficient. For the incident angle domain, a frequency of 10 GHz was selected.

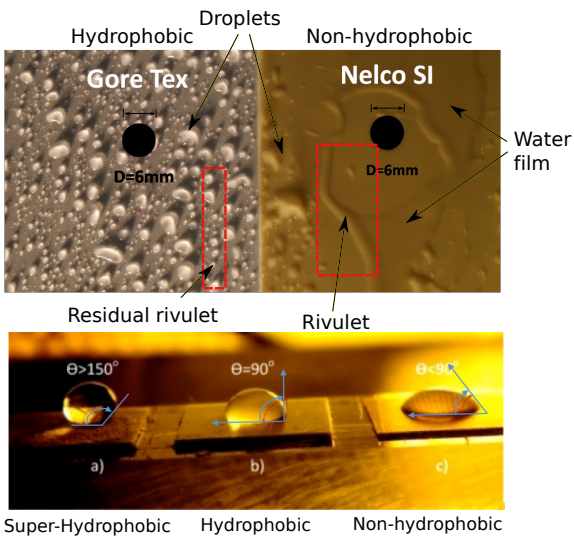


Figure 4: Water formation and radome skin surfaces

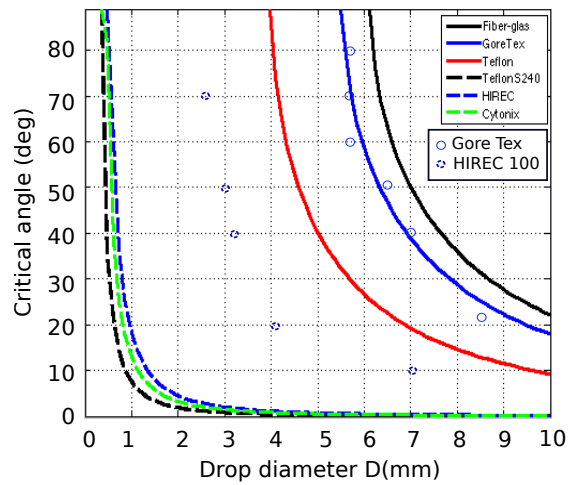


Figure 5: Critical angle versus tilted angle for radome skin surfaces

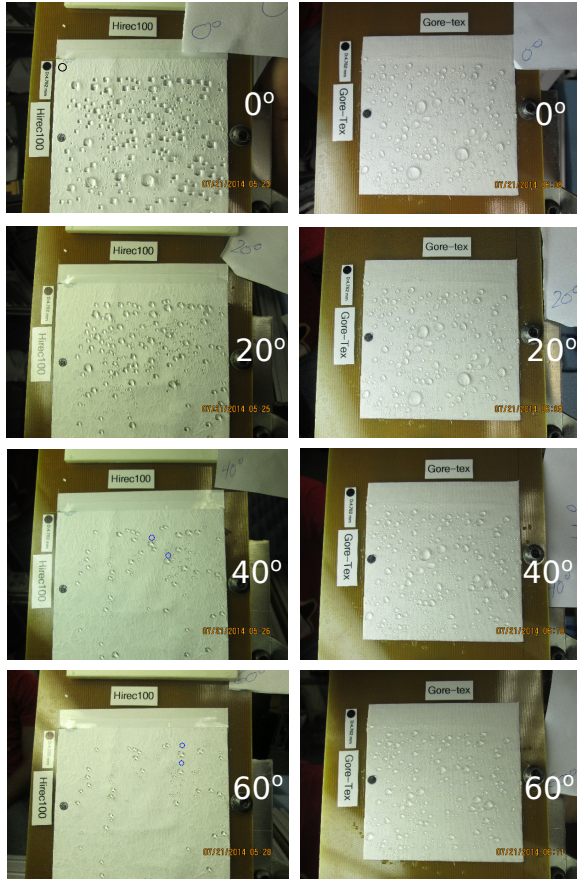


Figure 6: DSD for Hirec 100 and Gore Tex as function of tilted angle

IV. CONCLUSIONS

This paper presents an experimental approach to accurately characterize the scattering and propagation properties of multilayer radome. The design, fabrication and characterization of a seven-layer radome was discussed. The circuital equivalent transmission line method was

used to obtain the theoretical performance. Simulation performed in HFSS and measured results obtained in a customized RF chamber were used to validate the method proposed. The radome skin surface was implemented with non-hydrophobic, hydrophobic, and superhydrophobic materials. Characterization of water radome was evaluated as function of the radome geometry, position, and material. A experimental validation of the critical angle as function of the incident angle for two radome skin materials (Hydrophobic and superhydrophobic) was also presented.

REFERENCES

- Crane, R. K. (2002). Analysis of the effects of water on the ACTS propagation terminal antenna. *IEEE Transactions on Antennas and Propagation*, 50(7):954–965.
- Fenn, A. J. (1997). Measurements of wet radome transmission loss and depolarization effects in simulated rain at 20 GHz. In *10th International Conference on Antennas and Propagation, IEEE*, volume 1, pages 474–477. IEEE Conf. Publ. 436.
- Gibble, D. (1964). *Effect of rain on transmission performance of a satellite communication system*. 52 edition.
- Hirsch, H. and Grove, D. (1988). *Practical Simulation of Radar Antennas and Radomes*. Artech House.
- Kurri, M. and Huuskonen, A. (2008). Measurements of the transmission loss of a radome at different rain intensities. *Journal of Atmospheric and Oceanic Technology*, 25(1989):1590–1599.
- Salazar, J., Chandrasekas, V., Trabal, J., Siquera, P., Medina, R., Knapp, E., and McLaughlin, D. (2014). A Drop Size Distribution (DSD) -Based Model for Evaluating the Performance of Wet Radomes for Dual-Polarized Radars. *J. Atmos. Oceanic Technol.*, 31:2409–2430.
- Walton, J. (1970). *Radome Engineering Handbook: Design and Principles*. Marcel Dekker, Inc.
- Weigand, R. M. (1973). Performance of a Water-Repellent Radome Coating in an Airport Surveillance Radar. *Proceedings of the IEEE*, 61(July 1971):1167–1168.